New Phytologist

Research

A metabolite roadmap of the wood-forming tissue in *Populus tremula*

Ilka N. Abreu[1]*, Annika I. Johansson[1]*, Katarzyna Sokołowska[1,2], Totte Niittylä[1], Björn Sundberg[1,3], Torgeir R. Hvidsten[4,5], Nathaniel R. Street[4] and Thomas Moritz[1,6]

[1]Department of Forest Genetics and Plant Physiology, Swedish University of Agricultural Sciences, Umeå Plant Science Centre, Umeå S-901 83, Sweden; [2]Department of Plant Developmental Biology, Institute of Experimental Biology, Faculty of Biological Sciences, University of Wrocław, Kanonia 6/8, Wrocław 50-328, Poland; [3]Forest Division, Stora Enso AB, Nacka SE-13104, Sweden; [4]Department of Plant Physiology, Umeå Plant Science Centre, Umeå University, Umeå S-901 87, Sweden; [5]Faculty of Chemistry, Biotechnology and Food Science, Norwegian University of Life Sciences, Ås NO-1433, Norway; [6]The NovoNordisk Foundation Centre for Basic Metabolic Research, Faculty of Health and Medical Sciences, University of Copenhagen, Copenhagen DK-2200, Denmark

Author for correspondence:
Thomas Moritz
Tel: +46 (0)90786 8456
Email: Thomas.Moritz@slu.se

Received: *20 April 2020*
Accepted: *26 June 2020*

New Phytologist (2020) **228:** 1559–1572
doi: 10.1111/nph.16799

Key words: cambium, crysectioning, laser capture microdissection, metabolomics, *Populus*, wood.

Summary

- Wood, or secondary xylem, is the product of xylogenesis, a developmental process that begins with the proliferation of cambial derivatives and ends with mature xylem fibers and vessels with lignified secondary cell walls. Fully mature xylem has undergone a series of cellular processes, including cell division, cell expansion, secondary wall formation, lignification and programmed cell death. A complex network of interactions between transcriptional regulators and signal transduction pathways controls wood formation. However, the role of metabolites during this developmental process has not been comprehensively characterized.
- To evaluate the role of metabolites during wood formation, we performed a high spatial resolution metabolomics study of the wood-forming zone of *Populus tremula,* including laser dissected aspen ray and fiber cells.
- We show that metabolites show specific patterns within the wood-forming zone, following the differentiation process from cell division to cell death.
- The data from profiled laser dissected aspen ray and fiber cells suggests that these two cell types host distinctly different metabolic processes. Furthermore, by integrating previously published transcriptomic and proteomic profiles generated from the same trees, we provide an integrative picture of molecular processes, for example, deamination of phenylalanine during lignification is of critical importance for nitrogen metabolism during wood formation.

Introduction

With a growing demand for sustainable products, wood is becoming an increasingly important source of renewable biomass. From an industrial perspective, both the rate of wood formation (i.e. biomass production) and the quality of the wood are important traits. Future improvements in wood biomass production and the properties of wood, either by means of genetic engineering or by identifying elite lines using early markers for desirable wood characteristics, require a better understanding of the regulatory mechanisms underlying the wood developmental programme.

Wood is formed by the activity of the vascular cambium (hereafter referred to as cambium). The cambium consists of fusiform and ray initials, which give rise to the axial components of the woody stem: vessels, tracheids, fibers, companion cells and axial parenchyma (Fischer *et al.*, 2019). Differentiation is controlled by a complex network of interactions between transcriptional regulators and signal transduction pathways (Nakaba *et al.*, 2012; Ye & Zhong, 2015; Sundell *et al.*, 2017; Zinkgraf *et al.*, 2017; Chen *et al.*, 2019; Fischer *et al.*, 2019). Several transcriptomics studies of wood-forming tissue in *Populus* have shown that gene expression is tightly controlled in this tissue. By contrast, there have been very few studies profiling differences in metabolite concentrations between different cell types in the wood forming zone of angiosperm trees (Uggla *et al.*, 2001; Andersson-Gunneråas *et al.*, 2006; Immanen *et al.*, 2016; Ning *et al.*, 2018). Plant hormones are important as regulators of cambial activity and differentiation. There is evidence that auxin (indole 3-acetic acid; IAA) is a key organizer of cambial growth and vascular development; for example, there is a gradient of IAA concentration across the developing cambium, suggesting that this compound plays a role in positional signaling (Uggla *et al.*, 1996). However, there are also data suggesting that interactions between IAA and gibberellins (GAs) can play a part in

*These authors contributed equally to this work.

regulating secondary growth (Digby & Wareing, 1966; Telewski *et al.*, 1996; Bjorklund *et al.*, 2007). The importance of GAs in controlling cambial activity and xylem fiber length has been demonstrated using transgenic trees with altered GA biosynthesis or GA signaling (Eriksson *et al.*, 2000; Mauriat & Moritz, 2009; Mauriat *et al.*, 2011). It has also been shown that concentrations of bioactive GAs are high in the early expansion region of the wood-forming zone (Israelsson *et al.*, 2005), suggesting that they may play an important role in fiber tip growth. The role of cytokinins in wood formation has shown in transgenic cytokinin *Populus*, where increased cytokinin content stimulated cambial cell divisions and, interestingly, also led to increased cambial auxin concentration (Immanen *et al.*, 2016).

Metabolomics aims to identify and quantify the population of small molecules in a biological sample and to link this biochemical information to a phenotype or biological process (Fiehn, 2002; Goodacre *et al.*, 2004). In common with other assays of cellular activity, such as RNA-Seq, a major challenge of applying and interpreting metabolomics to developmental biology arises from the complexity of assaying tissues comprising multiple cell types, as is the case for wood. Sundberg and co-workers developed a tangential cryosectioning technique for the wood-forming zone in *Pinus silvestris* and *Populus*, enabling a highly spatially resolved characterization of IAA concentrations across the wood forming region (Uggla *et al.*, 1996). Since then the cryosectioning technique has been used to study many different aspects of wood development (Tuominen *et al.*, 1997; Uggla *et al.*, 1998; Hertzberg *et al.*, 2001; Uggla *et al.*, 2001; Schrader *et al.*, 2004; Courtois-Moreau *et al.*, 2009; Immanen *et al.*, 2016). While tangential sectioning is a powerful sampling technique to pool cells in similar stages of differentiation, it only indirectly permits resolving differences in cell-type specific programs. In particular, changes in ray cells might be masked by contributions from xylem vessel and fiber cells.

RNA sequencing of cryosections has dramatically improved our understanding of the transcriptional programme underlying wood development (Sundell *et al.*, 2017). However, since later processes of wood differentiation consist largely of dead cells, the short-lived nature of RNA means that transcriptomics provides only a limited view into xylem vessel and fiber formation at this terminal stage of the differentiation programme. Combining metabolomics and transcriptomics data has greatly enhanced the understanding of secondary wall deposition in xylem vessel-like cells (Li *et al.*, 2016; Ohtani *et al.*, 2016). While *Populus* wood has been extensively studied at the transcriptional level (e.g. Andersson-Gunneras *et al.*, 2006; Niculaes *et al.*, 2014), few studies have characterized metabolite profiles with high spatial resolution across wood forming tissues (Uggla *et al.*, 2001; Immanen *et al.*, 2016). To address this gap, we used 20 μm thick tangential sections spanning the active phloem–cambium–xylem developmental zones to produce a metabolic roadmap of wood-forming tissue in *Populus tremula* (aspen). We also included metabolomics data from laser capture dissected ray cells to provide cell-type specific data to overcome the limitations of tangential sectioning.

Materials and Methods

Plant material

The plant material consisted of 47-yr-old aspen (*Populus tremula* L.) trees growing in northern Sweden (lat. 64°21′N, long. 19°47′E). Five trees from the same clone were sampled on 7 July 2010. The results presented in this paper were obtained from the average of these trees. Blocks (2 × 10 cm) consisting of extraxylary tissues and a few annual rings were collected at a height of *c.* 3 m. The blocks were immediately frozen in liquid nitrogen and stored at −80°C until required for sectioning. The sections were obtained by centripetal tangential cryosectioning of *c.* 2 × 20 mm. Sampling and anatomical characterization of the tissues in each section was performed as described by Uggla *et al.* (1996, 1998). In parallel, one transverse hand section from the phloem to the annual ring was prepared from a specimen from Tree 1. This section was stained with safranin/alcian blue, washed in water and mounted in 50% glycerol.

Fibers and ray cell samples were isolated from 40 μm thick radial sections from the same aspen trees prepared on cryomicrotome (Leica CM3050 S, Nussloch, Germany) from a small wood block (*c.* 3 cm × 1 cm × 3 cm) containing phloem, cambium and a few annual growth rings (Supporting Information Methods S1).

Metabolite extraction

To reduce the number of samples and concentrate the ones in which metabolite content was expected to be low, sections from the phloem, expanding zone and the maturation zone were pooled. Samples from the cambial zone were kept as individual sections (Fig. S1).

All tagential sections, as well as ray and fiber cells were extracted in $CHCl_3$: MeOH : H_2O (1 : 3 : 1) according to the method described by Gullberg *et al.* (2004). For details, see Methods S2.

Gas chromatography–mass spectrometry (GC-MS) untargeted profiling

Dried extracts were first derivatized overnight at room temperature with methoxyamine (15 ng μl^{-1} pyridine), and thereafter with *N*-methyl-*N*-(trimethylsilyl)trifluoracetamid (MSTFA) with 1% trimethylchlorosilane (TMCS) for 1 h at room temperature. The derivatized extracts were analyzed as described previously (Gullberg *et al.*, 2004), using a Pegasus III GC-TOFMS (Leco Corp., St Joseph, MI, USA). All mass spectra (MS) files were exported in NetCDF format and processed using MATLAB R2011b (Mathworks, Natick, MA, USA) according to the method described by Jonsson *et al.* (2005) and using in-house scripts. The extracted mass spectra were identified by comparisons with retention index values and an in-house mass spectra library (Schauer *et al.*, 2005).

Liquid chromatography–mass spectrometry (LC-MS) untargeted profiling

The evaporated extracts were dissolved in methanol : water (50%, containing internal standards – see Methods S2) and the analysis was performed as described in Adolfsson *et al.* (2017).

The generated MS files were processed with an untargeted approach using MassHunter Profinder B.08.00 (Agilent Technologies Inc., Santa Clara, CA, USA) software. In addition, files generated from the LC–MS analysis of ray and fiber cells were also processed by targeted feature extraction, using all metabolites annotated in the wood sections as a database.

Data normalization was used to compensate for the resulting differences between pooled and un-pooled extracts. All data given here are the results of an average of profiling of five trees. Averaging and grouping of sections between the five trees was performed according to Table S3 (see later; sheet 'normalized 5 trees'), and based on distances from old phloem.

The strategy used for a systematic annotation of mass features present in the wood forming extracts was as follows (Fig. S2): (1) the automatic tandem mass spectrometry (autoMSMS) analysis was performed in the extracts using collision energy from 10 to 30 V. A manual search for the fragments *m/z* 195.0663, 193.0514, 137.0250 and 177.0560 in the MSMS spectra allowed selection of candidate metabolites for oligomer biosynthesis, which were thereafter compared with the spectral fragments described in Morreel *et al.* (2004, 2010) and Weng *et al.* (2008); (2) annotation of salicylates was performed according to the method described in Abreu *et al.* (2011). Their conjugated forms with phenylpropanoids were manually predicted by the interpretation of MSMS spectra; (3) mass searches of public databases of spectra were manually interpreted based on, among other descriptors, mass accuracy of fragments and neutral losses, and cross-checked with other public databases (www.plantcyc.org and KEGG pathways); (4) the MSMS networking (Wang *et al.*, 2016) was used to annotate metabolites with similar fragment patterns (Fig. S2c). All metabolites annotated in the aspen wood forming tissue are shown in Tables S1–S4.

Hormone analysis

Details for the analysis of IAA and cytokinin are described in Methods S3. In brief, the extracts were purified and fractionated using micro-SPE columns as described by Svacinova *et al.* (2012). The micro-SPE purified extracts containing IAA, after methylation followed by trimethylsilylation, were analysed using an Agilent 7000 GC/MS triple quadrupole mass spectrometer as described previously (Mauriat *et al.* 2011). The micro-SPE purified extracts containing cytokinins were analyzed in positive mode on an Agilent 6490 triple quadrupole mass spectrometer equipped with a high-performance liquid chromatography (HPLC)-Chip Cube MS Interface.

Statistical analysis

All univariate and multivariate statistical analyses were performed using Simca v13.0.2 (Umetrics, Umeå, Sweden) or Metabo Analyst 4.0 (https://www.metaboanalyst.ca/home.xhtml).

Data availability

Metabolomics data have been deposited in the European Molecular Biology Laboratory-European Bioinformatics Institute (EMBL-EBI) MetaboLights database (https://doi.org/10.1093/nar/gks1004; PubMed PMID: 23109552) with the identifiers MTBLS1796, MTBLS1797 and MTBLS1831. Files generated from the autoMSMS analysis were deposited under the study MTBLS1797 and characteristics fragments of the annotated metabolites are available in Table S4 and the Metabolite Annotation file (MTBLS1797). The complete dataset can be accessed here: https://www.ebi.ac.uk/metabolights.

Results and Discussion

In order to obtain a broad picture of metabolic changes occurring during wood development, we performed both untargeted metabolite profiling and targeted quantification of low-abundant phytohormones across the developing phloem and wood forming tissues in five clonal replicates of wild-growing, mature (47-yr-old) *P. tremula* (aspen) trees (Fig. S1). To additionally quantify metabolic activity in different cell types, we profiled laser dissected aspen ray and fiber cells isolated from 40 µm thick radial sections containing phloem, cambium and a few previous annual growth rings from the same aspen trees (Fig. S3).

Untargeted metabolomics data order wood samples according to the developmental gradient

Principal component analysis (PCA) score plots of the untargeted metabolomics data from the cryosections highlighted the complementary value of the two different techniques (GC-MS and LC-MS): The GC-MS profiling displays phloem and cambium samples as one cluster and expanding and mature xylem as a distinctly different second cluster (Fig. S4a). The LC-MS profiling, on the other hand, shows an ordered sample distribution from phloem, through cambium and expanding xylem, to mature xylem, suggesting clear metabolite gradients coinciding with the developmental gradient of these tissues (Fig. 1a) and revealing a more complex and differentiated composition of specialized metabolites in contrast to the primary metabolites detected by GC-MS. Furthermore, laser dissected ray and fiber cells were also discriminated in the metabolite profiling data (Fig. 2a), suggesting that these two cell types host distinctly different metabolic processes.

The aspen wood forming tissues show specific metabolite profiles

To evaluate the role of metabolites during wood formation we performed a high spatial resolution metabolomics study of the wood-forming zone. The untargeted GC-MS analysis identified 148 features, where the major metabolites are those involved in central carbon metabolism (e.g. sugars, organic acids, glycerols and amino acids) and phenolic metabolites (Table S1). Cluster analysis of those features revealed six specific clusters along the

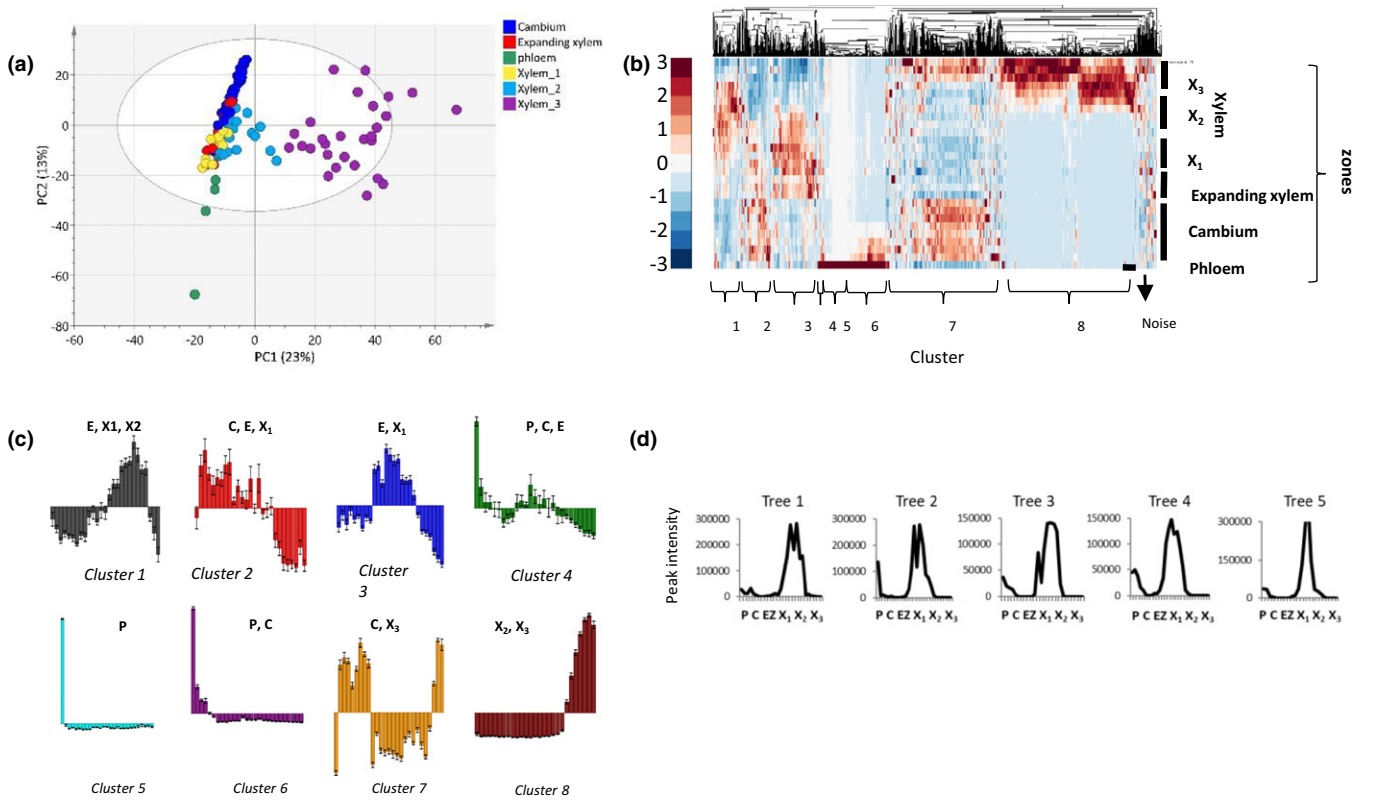

Fig. 1 Metabolite profiling by liquid chromatography quadrupole time-of-flight mass spectrometry (LC-QTOF-MS) of wood forming zones in five 47-yr-old aspen trees. (a) Principal component analysis (PCA) of metabolites generated from the profiling in negative ion mode. The scores plot (PC1 × PC2) shows the separation of the different samples from all trees. The PCA model generated 12 principal components with total explained variance (R2X(cum)) equal to 0.69. The predictive capacity by means of cross validation, Q2(cum), was 0.52; PC1 (23%) and PC2 (13%). Sample T04-28 was considered to be an outlier and was not included in the model. (b) Hierarchical clustering dendrogram and heatmap of the generated dataset showing eight metabolite clusters with distinct profiles across the wood sections. Clustering parameter, Euclidean distance; clustering method, unweighted average distance (UPGMA). (c) PCA models (UV-scaled, CV 95% error bars) with one component fitted for each cluster in (b). P, phloem; C, cambium; E, expanding xylem; X_1, X_2, X_3, mature xylem. The complete information from the liquid chromatography–mass spectrometry (LC-MS) generated data is provided in Supporting Information Table S2. (d) Concentrations of caffeoyl shikimate in all five trees as an example of data reproducibility, together with the PCA.

wood forming zones (containing metabolites abundant in xylem segment X_3, segments X_1/X_2, cambium, phloem/cambium, phloem/cambium/X_1, expanding/xylem segment X_1); however, fewer clusters were observed in the xylem segments X2 and X3 than in the early stages of wood development (Fig. S4b).

About 2240 features were detected by LC-MS, of which 399 metabolites were annotated (Tables S2, S3), and of those 156 were more specifically characterized according to their MS/MS fragmentation patterns (Table S4). Among the latter were phenolic glucosides (salicyloids, arbutin and salirepin), benzoates, flavonoids, cinnamate esters, oligomers and polar lipids (ceramides and galactolipids). Although there was some overlap between cambium and the expansion zone in the principal component analysis (PCA) score plot of the samples (Fig. 1a), an unsupervised hierarchical clustering analysis of detected features by LC-MS data revealed metabolite patterns distinct to each developmental stage (Fig. 1b). The clustering revealed eight distinct metabolite clusters across the wood-forming zone for untargeted LC-MS (Fig. 1b, for full description see Tables S2 and S3). Metabolites of cluster 1 had maximum abundance in the expanding and early xylem zones (X_1 and X_2). Such metabolites could be involved in the secondary wall deposition. In line with this, the same region showed an accumulation of monosaccharides in the GC-MS data (Table S1). RNA-seq analysis of the same wood sections identified several co-expression modules that were significantly enriched in genes involved in secondary cell wall biosynthesis, cell wall biosynthetic machinery and S-lignin and xylan biosynthesis (see Fig. 3 in Sundell *et al.*, 2017). Therefore, as metabolite cluster 1 coincides with those co-expression modules, the metabolites present in cluster 1 might be involved in this process. Cluster 2 was characterized by the accumulation of phenylalanine, caffeoyl glucoside, sucrose and glucoceramides in the cambium, expanding and X1 zones. These regions represent extensive primary wall synthesis, a process that requires sucrose as a substrate for cellulose biosynthesis. Interestingly, caffeoyl glucoside represents a monolignol precursor that might be transported from the expanding xylem to the mature xylem, where it could be hydrolyzed and incorporated into lignin. It should be emphasized that to able to verify this, flux data describing whether monolignol concentrations, including caffeoyl

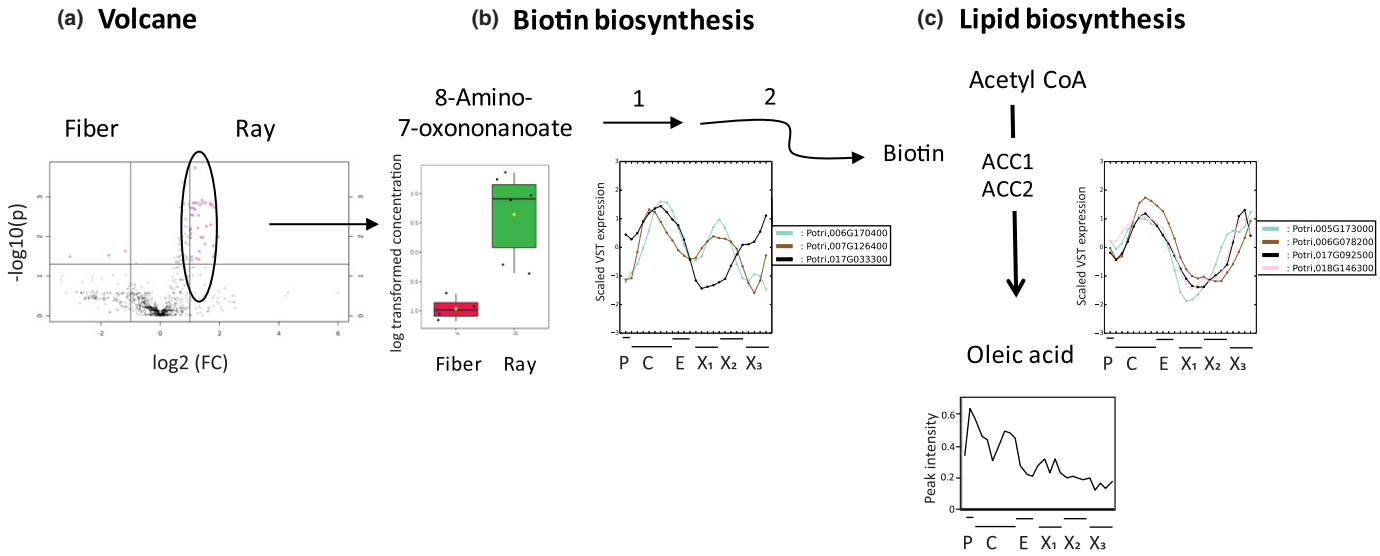

Fig. 2 Interaction between ray cells and aspen wood developing tissues for lipid biosynthesis. (a) Volcano plot comparing metabolite profiling of ray and fiber cells (fold change ≥ 1.5 and false discovery rate ($P \geq 0.05$); for details see Supporting Information Table S6. (b) Accumulation of 8-amino 7-oxononanoate in ray cells, an intermediate for biotin biosynthesis: increased expression of genes encoding the biotin biosynthetic enzymes in the cambium – *Potri.006G170400* (adenosylmethionine-8-amino-7-oxononanoate transaminases), *Potri.007G126400* (radical S-adenosyl methionine superfamily protein), *Potri.017G033300* (radical S-adenosyl methionine superfamily protein). (c) Biotin is a cofactor of acetyl coenzyme A (CoA) for oleic acid biosynthesis. Gene expression from AspWood (http://aspwood.popgenie.org).

glucoside, are static or due to rapid turnover, must be described. Cluster 3 showed that cinnamate esters, like caffeoyl and coumaroyl shikimate, accumulated in the expanding and X1 zones. Weng *et al.* (2008) demonstrated that such metabolites are an alternative resource for syringyl lignin in vascular plants. Salicin, a characteristic metabolite in cluster 4, was found predominately in the phloem, but was also present in smaller quantities in the cambium and expanding zone. By contrast, other salicyloids and their conjugated forms were found in clusters 5 and 6, with the former cluster representing metabolites exclusively present in the phloem and the later cluster containing metabolites typically present in the phloem and cambium. Besides salicyloids, the accumulation of flavonoids, trisaccharides and glutamate was typical for cluster 6. Cluster 7 metabolites (e.g. ascorbate, ellagic acid and galactolipids) accumulated in the cambium and mature xylem. Lignin-oligomers accumulated in the mature xylem (X2 and X3), as represented by cluster 8 (Fig. 1c).

Sundell *et al.* (2017) showed that gene expression clusters were highly reproducible in their four replicate trees, despite those being mature trees growing under natural conditions. In the present study, the metabolomics approach was performed in five replicates, where trees 1 to 4 were the exact same trees sampled by Sundell *et al.* (2017) and Obudulu *et al.* (2016). High reproducibility was also demonstrated from the metabolomics data by the PCA score plot and individual metabolite profiles (Fig. 1a and d, respectively), suggesting a high degree of genetic control of the processes. Using hierarchical clustering, Sundell *et al.* (2017) also identified eight main expression clusters, with some having a striking similarity with the metabolite clusters (Fig 1b, c). To test if metabolite and gene expression profiles indeed

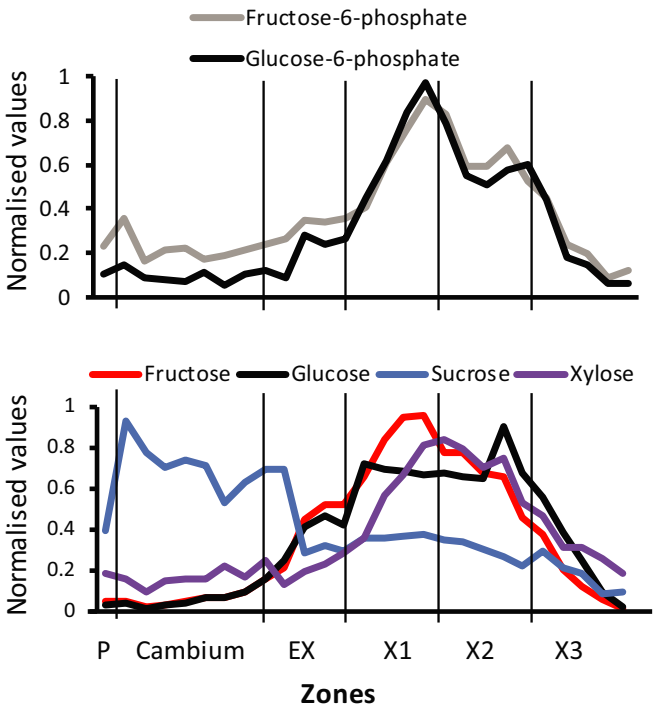

Fig. 3 Concentration profiles of cell wall sugars in wood forming zones of five 47-yr-old adult aspen trees: glucose-6-phosphate and fructose-6-phosphate; sucrose, glucose, fructose and xylose. The concentration profiles for each metabolite were normalized by setting the highest concentration found for that metabolite to 1.

overlap in wood forming tissue and if this overlap could be used to predict gene function, we examined more closely the biosynthesis of salicortin, a metabolite characteristic of cluster 5

(Fig. 1c). Salicortin, an abundant salicyloid accumulated in the phloem, is synthesized from the esterification of benzyl alcohol with 6-hydroxy-2-cyclohexen-one-carboxylate (HCH) by the hydrolase EC 4.2.1 (see https://pmn.plantcyc.org/; Fig. S5a). Bioinformatic predictions of EC 4.2.1 suggest 141 candidate genes in the *Populus* genome (https://www.pmn.plantcyc.org/), of which 99 are expressed in wood-forming tissue (http://aspwood.popgenie.org). We then compared the expression patterns of these 99 genes (Fig. S5b) with the salicortin concentrations in wood-forming tissue (Fig. S5c); only eight genes had highly overlapping gene expression with the salicortin metabolite profiles. Hence, these eight genes are likely candidates for EC4.2.1 function in salicortin biosynthesis. We believe such a comparative strategy could facilitate the identification of genes involved in secondary metabolism, especially when dealing with large gene families.

Aspen ray and fiber cells show distinct metabolite profile

The metabolite profiling by LC-MS performed on the laser-dissected ray and fiber cells, from an independent experiment, resulted in a detection of 1034 features and the annotation of 240 metabolites (Table S5). Interestingly, several metabolites – including salicyloids, benzoates, lignin oligomers, lignans and cinnamate esters – that were also characterized in the aspen wood forming tissues (Table S2) were present in the aspen ray and fiber cells. Although ray cells do not lignify during the present year's growing season, no differences in metabolites associated with lignification were observed between ray and fiber cells (Table S5). A recent study in Norway spruce showed that most of the shikimate and monolignol biosynthesis genes are equally expressed in parenchymal ray cells and upright tracheids, suggesting that ray parenchymal cells contribute to the lignification of upright tracheids (Blokhina *et al.*, 2019). Similarly, the presence of metabolites associated with lignification in ray cells may indicate that the ray cells contribute substrates for lignification to neighboring non-ray cells.

Enrichment of amino carboxylic acids (like 8-amino-7-oxononanoate, 8-amino methyl-7-oxononanoic acid, amino-oxoundecanoic acid and amino-oxododecanoic acid), dicarboxylic acids (suberic acid and decanedioic acid) and pyroglutamic acid was observed in aspen ray cells (Fig. 2b). These metabolites are involved in several specific metabolic processes and could aid understanding of some of the clusters generated by the GC-MS profiling in the wood forming tissues (Fig. S4). For example, 8-amino-7-oxononanoate is an intermediate of biotin biosynthesis, a vitamin required as a cofactor of enzymes involved in fatty acid and carbohydrate metabolism (Che *et al.*, 2003) (amongst others, acetyl-CoA carboxylase (ACCase)), gluconeogenesis (pyruvate carboxylase) and amino acid metabolism (methylcrotonyl-CoA carboxylase (MCCase) and propionyl CoA carboxylase). Curiously, increased expression of genes encoding the enzymes of biotin biosynthesis was found in the cambium and mature xylem of aspen wood forming tissues (http://aspwood.popgenie.org; Fig. 2b). These results suggest that the ray cells may provide intermediates for biotin biosynthesis in wood forming tissues, resulting in the biosynthesis of lipids and carbohydrates. Although biotin could not be detected by any of the analytical approaches used in this study, there was increased expression of four genes encoding lipid biosynthetic enzymes with biotin as a co-factor (ACCC.1, ACCC.2, HCS1 and a biotin carboxyl carrier) (Fig. 2c) in the cambium and mature xylem of the same plant material (http://aspwood.popgenie.org). These results are in line with the accumulation of lipids in the cambium (dodecanoic acid, adipic acid, arachidic acid, heptadecanoic acid, nonanoic acid, stearic acid and oleic acid) and cambium/mature xylem (1-Palmitoyl-*sn*-glycero-3-phosphocholine, ethanolamine, hexadecanoic acid, linoleic acid and beta-sitosterol), corresponding to clusters 3 and 6, respectively (see GC-heatmap order, Table S1). Lipid accumulation has previously been shown in the cambium, xylem ray cells, parenchymal pith and cortex by histochemical staining in stem sections of aspen (Grimberg *et al.*, 2018). Lipid accumulation was associated with the temporal coordination of growth cessation (Grimberg *et al.*, 2018), and storage of lipid droplets in the ray cells of *Populus* annual rings increases during autumn (Nakaba *et al.*, 2012). Our results indicate that the lipid accumulation in cambium and mature xylem depends on biotin biosynthesis, whose intermediates are provided by the ray cells.

Carbohydrates and cell wall formation

Once the dividing cells have reached their final dimensions in the region of cell expansion, secondary cell walls are deposited inside the primary wall. Formation of the secondary cell wall requires biosynthesis of polysaccharides, which in *Populus* mainly take the form of cellulose and xylan (Mellerowicz *et al.*, 2001). Sucrose, imported from the phloem and converted to uridine diphosphate (UDP)-glucose and fructose by sucrose synthase (SuSy) or glucose and fructose by invertases, is the main precursor for these polysaccharides (Mellerowicz *et al.*, 2001; Uggla *et al.*, 2001; Rende *et al.*, 2016). GC-MS metabolite profiling revealed differential patterns of sucrose, fructose and glucose (Fig. 3). The level of sucrose declined rapidly from the cambial tissue towards the expansion zone, whereas the monosaccharides glucose and fructose gradually increased, with maximum abundance in the zone of secondary wall formation (at around 800 µm from the cambium). The simultaneous increase in glucose and fructose may reflect increased invertase activity during secondary cell wall formation. Neutral invertases were shown to play an important role in supplying carbon to cellulose biosynthesis in aspen wood (Rende *et al.*, 2016). Roach *et al.* (2012) showed that fructokinases are important for converting the sucrose derived fructose into fructose-6-phosphate; fructokinases may also facilitate SuSy reaction towards UDP-glucose production. In our study, concentrations of fructose-6-phosphate, fructose and glucose-6-phosphate were highest in the early secondary wall deposition zone (Fig. 3), while fructokinase and SUS reach their highest activity in the expanding xylem of aspen wood (Roach *et al.*, 2017).

Xylose, which forms the sugar backbone of xylan, is the dominant hemicellulose of the secondary cell walls in *Populus* exhibited peak concentrations in the mature xylem, further away from

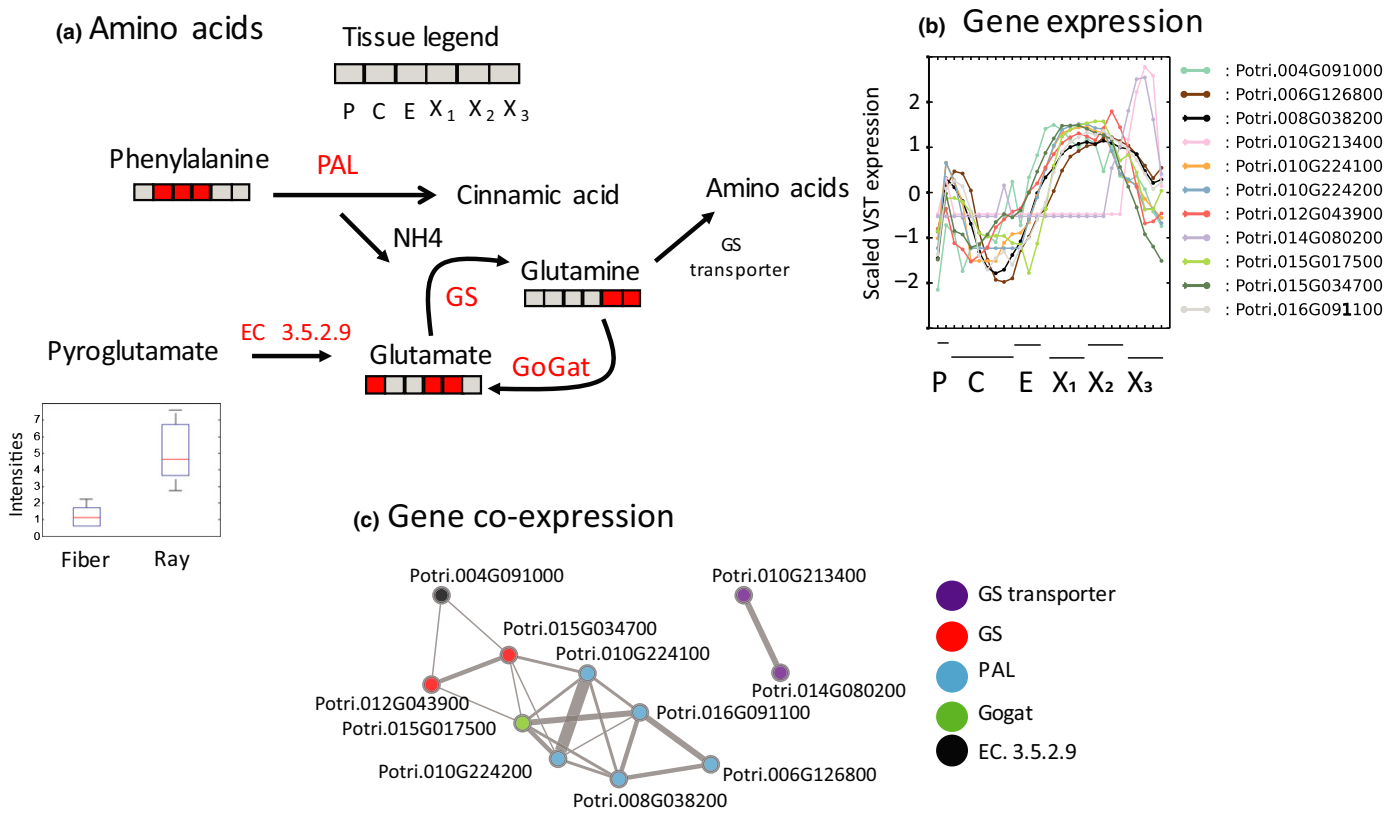

Fig. 4 Nitrogen metabolism in aspen wood forming zones. (a) Amino acid biosynthesis and accumulation of pyroglutamate in ray cells. Red colour shows where the metabolite is abundant. (b) Expression profiles of candidate genes across aspen wood formation and (c) their co-expression network: glutamine synthetase (GS) (*Potri.005G093200*, *Potri.012G043900*, *Potri.015G034700*), phenylalanine ammonia lyase (PAL) (*Potri.008G038200*, *Potri.010G224100*, *Potri.010G224200*, *Potri.016G091100*, *Potri.006G126800*), gogat (*Potri.015G017500*), EC. 3.5.2.9 (*Potri.004G091000*), GS transporter (*Potri.010G213400*, *Potri.014G080200*. Co-expressed genes are linked by lines, where thicker lines indicate stronger co-expression (higher correlation). The network has co-expression z-scores > 3.

the cambium than the other sugars, at a distance of about 800–1400 µm from the cambium. The increase in the level of xylose coincided with the formation of the secondary cell wall in this region.

Glutamine is the most abundant amino acid in the phloem and xylem

One of the most striking results related to amino acids was the large amount of glutamine found in the mature xylem. Glutamine abundance increased rapidly *c.* 800 µm from the cambium, exhibiting maximum abundance at about 1600 µm and then rapidly decreasing in the annual ring samples (Fig. 4a). The highest concentration of glutamine found in the xylem was 3–4 times higher than that found within the phloem. While glutamine was by far the most abundant amino acid found in the xylem, the highest abundance of glutamic acid was found in the phloem and expanding xylem (Table S1). Complementary to glutamine and glutamate, accumulation of phenylalanine was observed in the expansion zone (Fig. 4a). Phenylalanine is a substrate of phenylalanine ammonia lyase (PAL), and a starting point of the phenylpropanoid biosynthesis (e.g. monolignol biosynthesis), resulting in the production of cinnamate and elimination of ammonium. This may indicate that during lignification, ammonium released by PAL could be recycled and remobilized through incorporation into glutamate by glutamine synthetase (GS), resulting in glutamine (Fig. 4a). The incorporation of 2-oxoglutarate by glutamine oxoglutarate aminotransferase (GOGAT) results in the production of two glutamate molecules (Cantón *et al.*, 2005). Glutamine synthetase (GS) plays a central role in plant growth by fixing inorganic nitrogen into amino acids, with glutamine being the main transported amino acid in *Populus* (Tegeder & Masclaux-Daubresse, 2018). Interestingly, glutamate can also be synthetized from pyroglutamate (Paulose *et al.*, 2013. The amino acid data suggest that ammonium released by PAL during lignification is recycled by the GS/GOGAT system, that glutamine is transported for redistribution to the mature xylem and that pyroglutamate provides a glutamate supply. To test these hypotheses we searched for the gene expression patterns in the xylem zone of PAL, GS, GOGAT, 5-oxoprolinase (EC 3.5.2.9) and GS transporter in the AspWood database (http://aspwood.popgenie.org) (Fig. 4b). Genes encoding PAL, GS, GOGAT and 5-oxoprolinase all sharply peaked in the expanding and the early mature xylem, co-localizing with the highest abundance of glutamate. By contrast, the GS transporters were most highly expressed in the mature xylem, in the same region that glutamine accumulation was detected. Co-expression of those genes is shown in Fig. 4(c) and Fig. S6. The

GS transporter genes were co-expressed, as expected. However, the gene Potri.004G091000 (annotated as 5-oxoprolinase) was co-expressed with the two genes encoding for GS (Potri.012G043900, Potri.015G034700). *GOGAT* (Potri.015G017500) is central in the co-expression network and is co-expressed with several genes encoding for PAL and GS. Interestingly, proteomics analysis performed on sections from the same trees (Obudulu *et al.*, 2016) showed accumulation of GS (Potri.015G034700) in the expanding and early xylem X1 zone and both GOGAT (Potri.015G017500) and PAL (Potri.008G038200.1, Potri.010G224100.1, Potri.016G091100.1) in the mature xylem X_1–X_2 zones. Expression of PAL, GOGAT and GS genes was localized to the secondary wall deposition zone.

Together, these results suggest that the deamination of phenylalanine during lignification is of critical importance for nitrogen metabolism during wood formation in trees.

Secondary cell wall and lignification

As the secondary cell wall is formed, the cellulose and hemicellulose network is 'locked' by the lignification process. Lignin, a complex phenolic polymer, not only gives the plant mechanical support, but also contributes to plant defense and to the conductance of sap through lignified vascular elements (Mellerowicz *et al.*, 2001; Vanholme *et al.*, 2008). Three different hydroxycinnamyl alcohols, also known as monolignols, are used to build the polymeric lignins (i.e. *p*-coumaryl alcohol, coniferyl alcohol and sinapyl alcohol), and these monolignol units are referred to as guaiacyl (G), syringyl (S), and *p*-hydroxyphenyl (H) units (Vanholme *et al*, 2010). Several oligomers were identified in the wood forming tissues, where G and S were the most abundant units (Table S4). Oligomers containing additional units derived from 4OH benzoic acid (sp), vanillic acid (V) and 5OH coniferyl alcohol (5H) were also present, as previously described by Morreel *et al.* (2004). We could not observe any obvious patterns of monolignols, or clear sequential deposit of the different units during the xylem development. Most of the oligomers were detected in the mature xylem, with the exception of G(t8-O-4)G which was detected in the phloem and expanding xylem (Fig. 5). Lignification within the phloem has been observed in many species (Lourenco *et al.*, 2016), and both monolignol biosynthetic genes and peroxidase genes are expressed in the phloem of aspen wood (Sundell *et al.*, 2017). However, it is unclear whether the presence of G(t8-O-4)G in the phloem, but not in the xylem, points to contrasting lignin composition between these two tissues.

Cinnamates, phenylpropanoids derived from the deamination of phenylalanine, are the substrate for monolignol biosynthesis (Weng *et al.*, 2008). The metabolic profiling of wood forming tissue showed several cinnamates esterified with shikimate, glucose and phenolic glucosides (salicyloids, salirepin and arbutin; see Table S4). Those esters were accumulated differently across the tissues: caffeoyl and coumaroyl shikimate, which can be converted into S-units (Weng *et al.*, 2008), were accumulated in the expanding and early xylem (X_1); while coumaroyl, feruloyl and caffeoyl glucosides accumulated in the phloem, cambium and expanding/early xylem (Fig. 5). Accumulation of cinnamate esterified with salicyloids was observed in the phloem and cambium (clusters 5 and 6, Fig. 1 and Table S3). The accumulation of cinnamoyl salicortin in aspen leaves has been previously described (Abreu *et al.*, 2011), and Si *et al.* (2011) isolated caffeoyl salicin (populoside) and caffeoyl salirepin from the bark of *Populus ussuriensis*. Intriguingly, all the phenolic glucoside esters were present in phloem and cambium; however, salicin, salirepin and arbutin were present in clusters 4, 3 and 1, having maximum abundance around the expanding and early xylem region (Table S3; Fig 1). Phenolic glucosides were also detected in the ray cells (Table S5), potentially indicating that salicin, salirepin and arbutin esters are transported from the phloem to the expanding xylem. However, further studies, including the determination of metabolic fluxes, are needed to understand how the accumulation of these metabolites could be related to the lignification process.

Defense metabolites

Salicyloids are involved in herbivore resistance in *Populus* leaves (Abreu *et al.*, 2011) and are highly abundant in the bark (Si *et al.*, 2011). Twenty-nine salicyloids were annotated, ranging from basic to more complex structures in wood forming tissues (Table S4), and higher levels were found in the phloem and cambium (Fig. 5). Some of them, such as salicortin and its derivatives (HCH-salicortin and feruloyl-salicortin), were only present in the phloem, while others were found at high concentrations in the phloem and the outermost cambium sections, with rapidly decreasing concentrations towards the expansion zone, whereas salicin was found distributed from phloem until the early xylem (X1) tissues (Fig. 5). By contrast, high concentrations of *p*-Benzoic acid were observed in the expanding and early xylem tissues (Tables S1, S3). We also observed the presence of oligomers containing *p*-benzoate (V unit), which has been previously characterized in *Populus* lignin (Morreel *et al.*, 2004).

In *Populus nigra*, the biosynthesis of HCH moiety of salicortin has a phenylpropanoid origin, while the salicyl moiety has a benzaldehyde origin (Babst *et al.*, 2010). Similarly, in *Salix pentandra* salicin biosynthesis has a benzoic acid route (Ruuhola & Julkunen-Tiitto, 2003). Benzoic acid (BA) can be synthetized though the shikimate/chorismate pathway in the plastids (Wildermuth, 2006), or the phenylalanine (Phe)/cinnamate (CA) route in the cytoplasm (Widhalm & Dudareva, 2015). Its biosynthesis from the Phe/CA in plants can follow two routes: either a coenzyme A (CoA)-dependent β-oxidative pathway or a non-β-oxidative pathway (Fig. 6a). The CA produced by the deamination of Phe is converted to BA after the shortening of two carbons, which can happen through one or both CoA dependent pathways (Qualley *et al.*, 2012).

As salicin is found in the early xylem, it is possible that salicylates and *p*-benzoate are produced through the same biosynthetic route. To this end, the expression of genes coding for the enzymes from the CoA dependent β-oxidative and non-β-oxidative pathway (Fig. 6a) were examined in the AspWood database

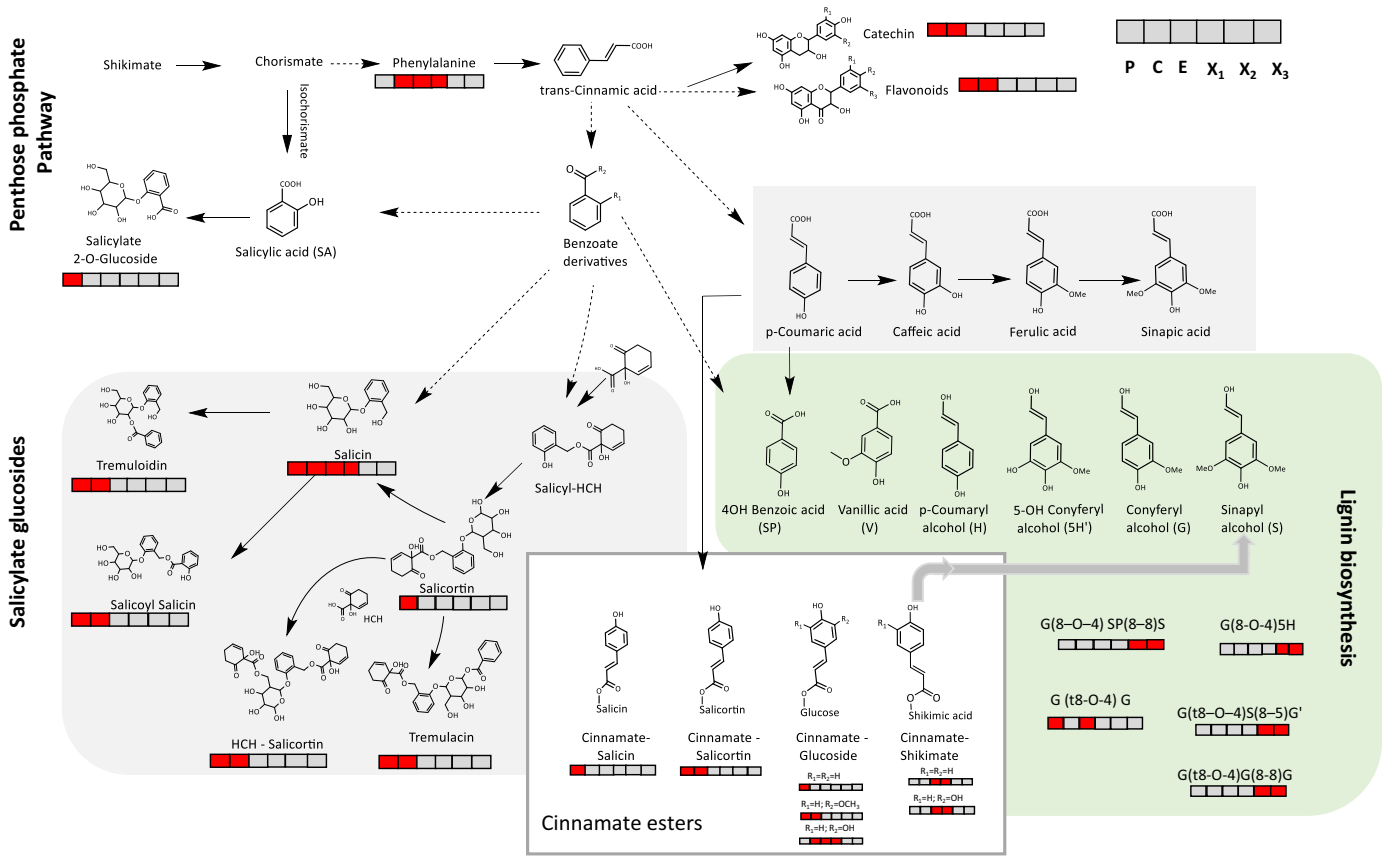

Fig. 5 Overview of phenolic metabolite gradient across the aspen wood forming zones. Red colour shows where the metabolite is abundant. P, phloem; C, cambium; E, expanding xylem; X_1, X_2, X_3, mature xylem.

(Sundell *et al.*, 2017). Some of the enzymes contained several predicted genes (Fig. 6b), and the ones with an expression profile matching that of the metabolite accumulation are shown in Fig. 6(c). The five genes encoding PAL ('1' in Fig. 6c) were expressed in the phloem and expanding xylem; and the genes encoding the enzymes CA/4-coumarate-CoA ligase ('2') and benzaldehyde dehydrogenase ('3'), from which *p*-benzoate/BA is produced through the non-oxidative pathway (Fig. 6a), were expressed in the mature xylem (Fig. 6c). These results agreed with the accumulation of *p*-benzoate and oligomers containing V units in the same tissues (Table S4; Fig. 5). High expression of the peroxisomal cinnamate-CoA ligase ('2*'), benzyl alcohol *O*-benzoyltransferase ('4') and a benzoate dehydrogenase ('5') was observed in the phloem, from which BA is produced through a β-oxidative pathway. The co-expression of all annotated genes showed three clusters: PAL, genes involved in the β-oxidative pathway, and genes from the non-oxidative pathway (Fig. 6d).

The results from the gene expression (Fig. 6) and the metabolite accumulation (Fig. 5) suggest that salicyloids are produced through the β-oxidative route, while the *p*-benzoates are produced by the non-enzymatic route. Therefore, the lignification and defense metabolism are not competitive processes. However, the high concentrations of salicyloids esterified with cinnamates in the phloem and salicin in the expanding xylem may suggest a tradeoff between the two metabolic processes.

Hormones and the vascular cambium

Plant hormones such as IAA, GA and cytokinins are key regulators of growth and development. To explore hormone levels across the wood-forming zone, and in particular across the cambial region, the content of IAA and cytokinins in each section was determined using quantitative GC-MS and LC-MS methods.

As in earlier studies by Uggla *et al.* (1996, 1998, 2001) and Tuominen *et al.* (1997), a steep concentration gradient in IAA across the vascular cambium was observed (Fig. 7). Uggla *et al.* (2001) showed that the radial gradient of IAA in latewood-forming tissue was steeper than the gradient in early wood-forming tissue. They also found that the cell division activity was not affected by a decrease in IAA concentration. The presence of a gradient therefore suggests that IAA may act as a positional marker or morphogen, possibly by controlling the amount of time each cambial derivative remains in the different developmental zones within the cambial region (Sundberg *et al.*, 2000). The role of IAA as a morphogen has been debated, and Benkova *et al.* (2009) instead introduced the concept of the morphogenic trigger. Nevertheless, other signals are also likely to be involved in the regulation of the rate of cell division, including auxin, as discussed by Bhalerao & Fischer (2014).

The concentrations of zeatin riboside (ZR), a precursor of the biologically active molecule zeatin, followed the same steep gradient over the vascular cambium as IAA (Fig. 7). Although the

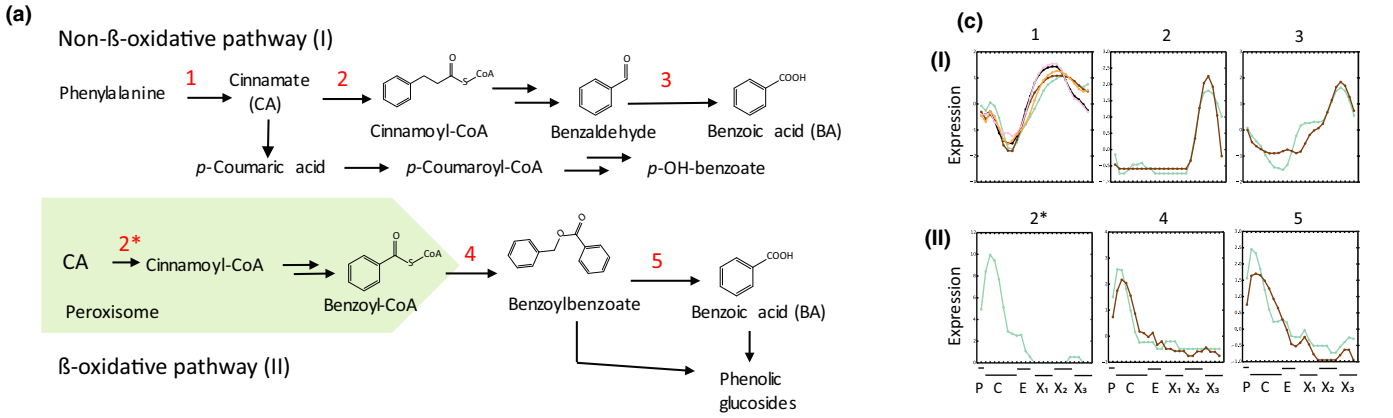

(b)

Step	E.C.	Reaction	Predicted	Description	"Putative" Gene
Non-ß-Oxidative (CoA-dependent)					
1	4.3.1.24/25	Phe → CA	5	PHE ammonia lyase 1	Potri.006G126800
				PHE ammonia lyase 1	Potri.008G038200
				PHE ammonia lyase 1	Potri.010G224100
				PHE ammonia lyase 1	Potri.010G224200
				PHE ammonia lyase 1	Potri.016G091100
2	6.2.1	CA → Cinnamoyl - CoA	20	AMP -dependent synthetase/ ligase	Potri.016G034800
				AMP -dependent synthetase/ ligase	Potri.006G036200
3	1.2.1.28	Benzaldehyde → Benzoate	15	Aldehyde dehydrogenase	Potri.001G167100
				Aldehyde dehydrogenase 3F1	Potri.007G017100
ß-Oxidative (CoA-dependent)					
2*	6.2.1	CA → C innamoyl - CoA	20	Peroxisomal 3 -ketoacyl - CoA thiolase 3	Potri.004G082000
4	2.3.1.196	Benzoyl -CoA → Benzylbenzoate	21	Acyl -transferase	Potri.013G074400
				Acyl -transferase	Potri.013G074500
5	Unknown	Benzylbenzoate → BA	106	Aldehyde dehydrogenase	Potri.018G075000
				Carboxyesterase	Potri.004G101400

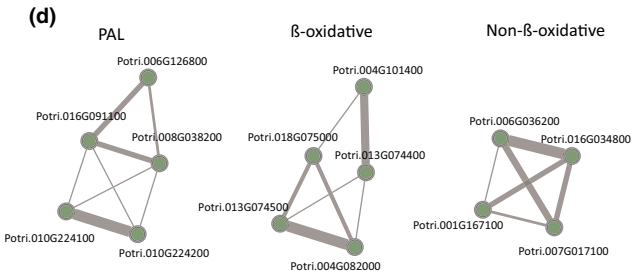

Fig. 6 Tradeoff expression of genes involved in defense and lignification in aspen wood forming zones. (a) Non-β-oxidative and -β-oxidative pathways for benzoate biosynthesis. (b) Gene annotation from AspWood (Sundell *et al*, 2017): 1, phenylalanine ammonia lyase (PAL); 2, cinnamate/4-coumarate-CoA ligase; 3, benzaldehyde dehydrogenase; 4, benzyl alcohol *O*-benzoyltransferase; 5, benzoate dehydrogenase. (c) Gene expression, and (d) co-expression of annotated genes. Co-expressed genes are linked by lines, where thicker lines indicate stronger co-expression (higher correlation). The network has co-expression z-scores > 3.

amount of zeatin was below the limits of detection in this experiment, the concentrations of ZR indicate that there was a concentration gradient of zeatin-type cytokinins across the vascular cambium. The concentrations of isopentenyl adenosine (iPA) were lower than those of ZR; however, iPA also showed a distinct peak in the cambial region, which overlapped with the ZR peak (Fig. 7). The concentrations of isopentenyl adenosine 5′ monophosphate (iPMP), a precursor of iPA, on the other hand, did not peak in the cambial region; instead, they were found to be fairly uniform up to a point *c.* 800 µm from the cambium, and then followed a steady decline towards the annual ring. A peak in cytokinin concentrations in the vascular cambium was anticipated, since several studies have demonstrated a role for cytokinin in controlling the rate of cell division within the cambium (Matsumoto-Kitano *et al.*, 2008; Nieminen *et al.*, 2008; Immanen *et al.*, 2016). Nieminen *et al.* (2008) showed that the number of cells in the cambial layer was lower in transgenic lines of *Populus* with a reduced concentration of active cytokinins, indicating that cytokinin concentrations have an impact on the rate of cell division. They also measured the expression of the cytokinin receptor family across the cambial region and found that the peak in expression levels coincides with the expression of a marker gene for cambial cell identity. In the present study, a closer examination of the pattern of ZR and IAA concentrations in the cambial region revealed that the peak in the ZR gradient is slightly shifted towards the phloem side in comparison to the IAA peak. This pattern was the same in all trees analyzed (Table S6). Similar patterns of cytokinins in the wood forming tissue in *P. tremula* × *P. tremuloides* have also been shown by Immanen *et al.* (2016). Altogether, this observation suggests that cytokinins are involved in regulating cell division whereas, IAA acts as a morphogen, providing the cambial region with positional information. The cytokinin peak may indicate the position of the cambial initials, which previous studies have suggested are located towards the phloem side of the cambial region (Schrader *et al.*, 2004; Nilsson *et al.*, 2008).

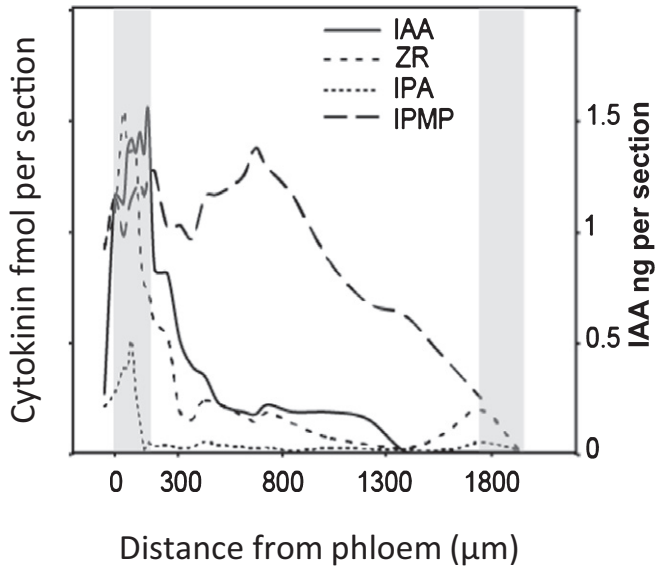

Fig. 7 Plant hormones in the aspen wood forming zone (tree 1). Indole 3-acetic acid (IAA; ng per section); cytokinins (fmol per section): zeatin riboside (ZR), isopentenyl adenosine (iPA), isopentenyl adenosine 5′ monophosphate (IPMP). The left-hand and right-hand grey areas represent the cambium and annual ring zones, respectively, and the distance (µm) from the first cambium sample is indicated on the *x*-axis. Individual concentrations for all five adult trees are shown in Supporting Information Table S3.

Conclusions

In the present study we have shown specific patterns of metabolites, including signaling compounds, in different regions of the wood-forming zone in *P. tremula*. Many of these patterns can be explained based on the developmental processes occurring within these regions, for example in the cambium (summarized in Fig. 8). However, interpretation of metabolomics data from the wood development zone is complicated by the fact that in addition to developmental processes, the transport of nutrients and secondary metabolites within the phloem and xylem must also be considered. The xylem transpiration stream that transports water and nutrients from the root to the shoot makes a major contribution to the metabolites in the samples from mature wood, and these nutrients and metabolites do not reflect the developmental state of the wood cells in this region. As well as the transpiration stream, these sections also contain ray cells, which stay alive for years and are metabolically active, in contrast to the dead xylem vessels and fibers. Hence there are at least three possible reasons for increases in metabolite content in the mature dead wood zone. The first possibility is that the concentration of the metabolite is increasing as a result of xylogenesis, that is, the metabolite is involved in molecular developmental processes within the wood cells. The second is that the increase is due to the xylem transpiration stream that passes through the region. This probably explains the three- to four-fold increase in glutamine concentrations observed in the mature xylem tissue compared to the phloem tissue. The third possible explanation is that the increase in metabolite content may be due to the metabolic activity of the ray cells.

The data presented here indicate that cambial activity, cell expansion and secondary cell wall thickening are tightly coupled processes, as suggested by Uggla *et al.* (2001). In the current study both cytokinin and IAA showed distinct peaks in the cambial region. The concentration maximum for IAA was found to be towards the xylem side of this region, whereas the maximum for cytokinins was further towards the phloem. Altogether, these findings suggest that plant hormones such as auxins and cytokinins have important roles in controlling cell division and position in the cambium region. The newly formed xylem vessels and fibers elongate to reach their final dimensions in the expansion zone, and this is reflected in a dramatic increase in the concentrations of glucose,

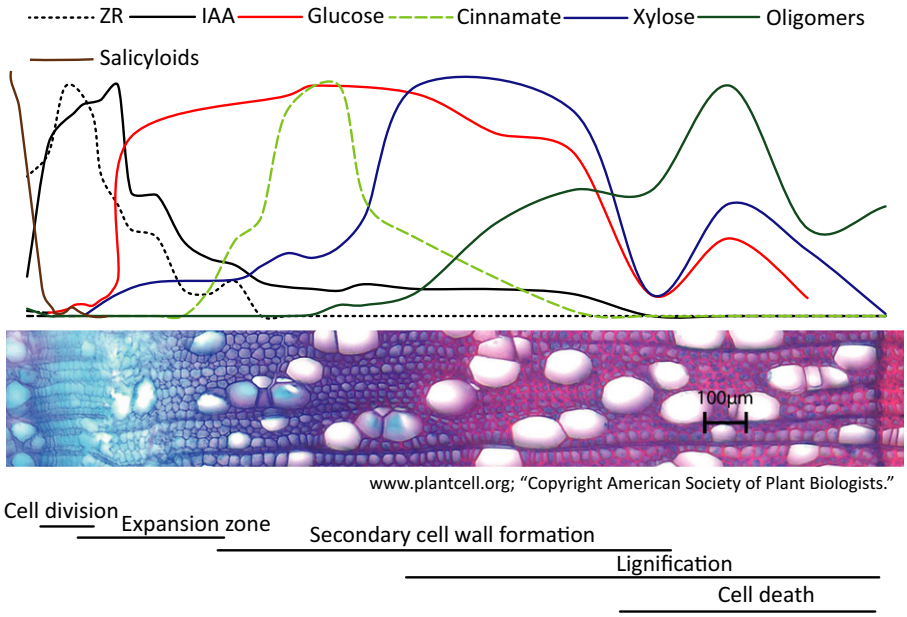

Fig. 8 Model for major metabolic shifts during aspen wood formation. Transverse wood section from Sundell *et al*. (2017).

which is the monomeric subunit of cellulose, the main polysaccharide of the primary wall. When the fibers and vessels have attained their final dimensions in the expansion zone, the secondary cell wall is formed inside the primary wall (Mellerowicz *et al.*, 2001). We found that concentrations of xylose, the subunit of the hemicellulose xylan, increase as the glucose concentration starts to decrease, marking the transition from primary cell wall to secondary cell wall formation. Oligomers were found to accumulate after the xylose peak, indicating that lignification occurs at a later stage of differentiation compared to formation of the secondary cell wall. However, accumulation of the monolignol precursors of lignin occurred before the accumulation of xylose, suggesting that biosynthesis of the monolignols begins during the transition from primary to secondary cell wall formation, whereas polymerization occurs at a later stage of differentiation.

Acknowledgements

We thank the Swedish Metabolomics Centre for technical support. Dr Moritz Wagner, Agilent Technologies, Waldbronn, Germany, is acknowledged for help setting up the HPLC-Chip Cube-MSMS analysis. This study was financially supported by the Carl Tryggers foundation, the Kempe Foundation, Formas, Knut & Alice Wallenberg Foundation and corresponding cofunding from the Swedish University of Agricultural Sciences. This work was also supported by financial contributions from Bio4Energy (Swedish Programme for Renewable Energy), Vinnova (the Swedish Governmental Agency for Innovation Systems) and KAW (The Knut and Alice Wallenberg Foundation) to Umeå Plant Science Centre.

Author contributions

INA, AIJ, TN, BS and TM designed the research plans; INA and AIJ performed the metabolomics experiments; KS performed the laser dissection experiments; AIJ and INA performed statistical analysis; INA, AIJ, TN, TRH, NRS and TM interpreted the results. All authors were involved in the writing process. TM supervised the research. INA and AIJ contributed equally to this work.

ORCID

Ilka N. Abreu https://orcid.org/0000-0003-4728-0161
Torgeir R. Hvidsten https://orcid.org/0000-0001-6097-2539
Thomas Moritz https://orcid.org/0000-0002-4258-3190
Totte Niittylä https://orcid.org/0000-0001-8029-1503
Katarzyna Sokołowska https://orcid.org/0000-0002-5874-207X
Nathaniel R. Street https://orcid.org/0000-0001-6031-005X

References

Abreu IN, Ahnlund M, Moritz T, Albrectsen BR. 2011. UHPLC-ESI/TOFMS determination of salicylate-like phenolic gycosides in *Populus tremula* leaves. *Journal of Chemical Ecology* **37**: 857–870.

Adolfsson L, Nziengui H, Abreu IN, Šimura J, Beebo A, Herdean A, Aboalizadeh J, Široká J, Moritz T, Novák O *et al.* 2017. Enhanced secondary- and hormone metabolism in leaves of Arbuscular Mycorrhizal *Medicago truncatula*. *Plant Physiology* **175**: 392–411.

Andersson-Gunneras S, Mellerowicz EJ, Love J, Segerman B, Ohmiya Y, Coutinho PM, Nilsson P, Henrissat B, Moritz T, Sundberg B. 2006. Biosynthesis of cellulose-enriched tension wood in *Populus*: global analysis of transcripts and metabolites identifies biochemical and developmental regulators in secondary wall biosynthesis. *The Plant Journal* **45**: 144–165.

Babst BA, Harding SA, Tsai CJ. 2010. Biosynthesis of phenolic glycosides from phenylpropanoid and benzenoid precursors in *Populus*. *Journal of Chemical Ecology* **36**: 286–297.

Benkova E, Ivanchenko MG, Friml J, Shishkova S, Dubrovsky JG. 2009. A morphogenetic trigger: is there an emerging concept in plant developmental biology? *Trends in Plant Science* **14**: 189–193.

Bhalerao RP, Fischer U. 2014. Auxin gradients across wood-instructive or incidental? *Physiologia Plantarum* **151**: 43–51.

Björklund S, Antti H, Uddestrand I, Moritz T, Sundberg B. 2007. Cross-talk between gibberellin and auxin in development of *Populus* wood: gibberellin stimulates polar auxin transport and has a common transcriptome with auxin. *The Plant Journal* **52**: 499–511.

Blokhina O, Laitinen T, Hatakeyama Y, Delhomme N, Paasela T, Zhao L, Street NR, Wada H, Kärkönen A, Fagerstedt K. 2019. Ray parenchymal cells contribute to lignification of tracheids in developing xylem of Norway spruce. *Plant Physiology* **181**: 1552–1572.

Cantón FR, Suárez MF, Cánovas FM. 2005. Molecular aspects of nitrogen mobilization and recycling in trees. *Photosynthesis Research* **83**: 265–278.

Che P, Weaver LM, Wurtele ES, Nikolau BJ. 2003. The role of biotin in regulating 3-methylcrotonyl-coenzyme A carboxylase expression in Arabidopsis. *Plant Physiology* **131**: 1479–1486.

Chen H, Wang JP, Liu H, Li H, Lin YJ, Shi R, Yang C, Gao J, Zhou C, Li Q *et al.* 2019. Hierarchical transcription factor and chromatin binding network for wood formation in black cottonwood (*Populus trichocarpa*). *Plant Cell* **31**: 602–626.

Courtois-Moreau CL, Pesquet E, Sjödin A, Muñiz L, Bollhöner B, Kaneda M, Samuels L, Jansson S, Tuominen H. 2009. A unique program for cell death in xylem fibers of *Populus* stem. *The Plant Journal* **58**: 260–274.

Digby J, Wareing PF. 1966. Effect of applied growth hormones on cambial division and differentiation of cambial derivatives. *Annals of Botany* **30**: 539.

Eriksson ME, Israelsson M, Olsson O, Moritz T. 2000. Increased gibberellin biosynthesis in transgenic trees promotes growth, biomass production and xylem fiber length. *Nature Biotechnology* **18**: 784–788.

Fiehn O. 2002. Metabolomics–the link between genotypes and phenotypes. *Plant Molecular Biology* **48**: 155–171.

Fischer U, Kucukoglu M, Helariutta Y, Bhalerao RP. 2019. The dynamics of cambial stem cell activity. *Annual Review of Plant Biology* **70**: 293–319.

Goodacre R, Vaidyanathan S, Dunn WB, Harrigan GG, Kell DB. 2004. Metabolomics by numbers: acquiring and understanding global metabolite data. *Trends in Biotechnology* **22**: 245–252.

Grimberg A, Lager I, Street NR, Robinson KM, Marttila S, Mahler N, Ingvarsson PK, Bhalerao RP. 2018. Storage lipid accumulation is controlled by photoperiodic signal acting via regulators of growth cessation and dormancy in hybrid aspen. *New Phytologist* **219**: 619–630.

Gullberg J, Jonsson P, Nordstrom A, Sjostrom M, Moritz T. 2004. Design of experiments: an efficient strategy to identify factors influencing extraction and derivatization of *Arabidopsis thaliana* samples in metabolomic studies with gas chromatography/mass spectrometry. *Analytical Biochemistry* **331**: 283–295.

Hertzberg M, Aspeborg H, Schrader J, Andersson A, Erlandsson R, Blomqvist K, Bhalerao R, Uhlén M, Teeri TT, Lundeberg J *et al.* 2001. A transcriptional roadmap to wood formation. *Proceedings of the National Academy of Sciences, USA* **98**: 14732–14737.

Immanen J, Nieminen K, Smolander OP, Kojima M, Alonso Serra J, Koskinen P, Zhang J, Elo A, Mähönen AP, Street N *et al.* 2016. Cytokinin and auxin display distinct but interconnected distribution and signaling profiles to stimulate cambial activity. *Current Biology* **26**: 1990–1997.

Israelsson M, Sundberg B, Moritz T. 2005. Tissue-specific localization of gibberellins and expression of gibberellin-biosynthetic and signaling genes in wood-forming tissues in aspen. *The Plant Journal* **44**: 494–504.

Jonsson P, Johansson AI, Gullberg J, Trygg J, Jiye A, Grung B, Marklund S, Sjöström M, Antti H, Moritz T. 2005. High-throughput data analysis for detecting and identifying differences between samples in GC/MS-based metabolomic analyses. *Analytical Chemistry* **77**: 5635–5642.

Li Z, Omranian N, Neumetzler L, Wang T, Herter T, Usadel B, Demura T, Giavalisco P, Nikoloski Z, Persson S. 2016. A transcriptional and metabolic framework for secondary wall formation in Arabidopsis. *Plant Physiology* **172**: 1334–1351.

Lourenco A, Rencoret J, Chemetova C, Gominho J, Gutierrez A, Del Rio JC, Pereira H. 2016. Lignin composition and structure differs between xylem, phloem and phellem in *Quercus suber* L. *Frontiers Plant Science* **27**: 1612.

Matsumoto-Kitano M, Kusumoto T, Tarkowski P, Kinoshita-Tsujimura K, Václavíková K, Miyawaki K, Kakimoto T. 2008. Cytokinins are central regulators of cambial activity. *Proceedings of the National Academy of Sciences, USA* **105**: 20027–20031.

Mauriat M, Moritz T. 2009. Analyses of GA20ox- and GID1-over-expressing aspen suggest that gibberellins play two distinct roles in wood formation. *The Plant Journal* **58**: 989–1003.

Mauriat M, Sandberg LG, Moritz T. 2011. Proper gibberellin localization in vascular tissue is required to control auxin-dependent leaf development and bud outgrowth in hybrid aspen. *The Plant Journal* **67**: 805–816.

Mellerowicz E, Baucher M, Sundberg B, Boerjan W. 2001. Unravelling cell wall formation in the woody dicot stem. *Plant Molecular Biology* **47**: 239–274.

Morreel K, Kim H, Lu F, Dima O, Akiyama T, Vanholme R, Niculaes C, Goeminne G, Inzé D, Messens E *et al.* 2010. Mass spectrometry-based fragmentation as an identification tool in lignomics. *Analytical Chemistry* **82**: 8095–8105.

Morreel K, Ralph J, Kim H, Lu F, Goeminne G, Ralph S, Messens E, Boerjan W. 2004. Profiling of oligolignols reveals monolignol coupling conditions in Lignifying poplar xylem. *Plant Physiology* **136**: 3537–49.

Nakaba S, Begum S, Yamagishi Y, Jin H-O, Kubo T, Funada R. 2012. Differences in the timing of cell death, differentiation and function among three different types of ray parenchyma cells in the hardwood *Populus sieboldii* × *P. grandidentata*. *Trees* **26**: 743–750.

Niculaes C, Morreel K, Kim H, Lu FC, Mckee LS, Ivens B, Haustraete J, Vanholme B, Rycke RD, Hertzberg M *et al.* 2014. Phenylcoumaran benzylic ether reductase prevents accumulation of compounds formed under oxidative conditions in poplar xylem. *Plant Cell* **26**: 3775–3791.

Nieminen K, Immanen J, Laxell M, Kauppinen L, Tarkowski P, Dolezal K, Tahtiharju S, Elo A, Decourteix M, Ljung K *et al.* 2008. Cytokinin signaling regulates cambial development in poplar. *Proceedings of the National Academy of Sciences, USA* **105**: 20032–20037.

Nilsson J, Karlberg A, Antti H, Lopez-Vernaza M, Mellerowicz E, Perrot-Rechenmann C, Sandberg G, Bhalerao RP. 2008. Dissecting the molecular basis of the regulation of wood formation by auxin in hybrid aspen. *Plant Cell* **20**: 843–855.

Ning K, Ding C, Zhu W, Zhang W, Dong Y, Shen Y, Su X. 2018. Comparative metabolomic analysis of the cambium tissue of non-transgenic and multi-gene transgenic poplar (*Populus* × *euramericana* 'Guariento'). *Frontiers in Plant Science* **9**: 1201.

Obudulu O, Bygdell J, Sundberg B, Moritz T, Hvidsten TR, Trygg J, Wingsle G. 2016. Quantitative proteomics reveals protein profiles underlying major transitions in aspen wood development. *BMC Genomics* **17**: 119.

Ohtani M, Morisaki K, Sawada Y, Sano R, Uy ALT, Yamamoto A, Kurata T, Nakano Y, Suzuki S, Matsuda M *et al.* 2016. Primary metabolism during biosynthesis of secondary wall polymers of protoxylem vessel elements. *Plant Physiology* **172**: 1612–1624.

Paulose B, Chhikara S, Coomey J, Jung H, Vatamaniuk O, Dhankhera OP. 2013. A γ-glutamyl cyclotransferase protects Arabidopsis plants from heavy metal toxicity by recycling glutamate to maintain glutathione homeostasis. *Plant Cell* **25**: 4580–95.

Qualley AV, Widhalm JR, Adebesin F, Kish CM, Dudareva N. 2012. Completion of the core β-oxidative pathway of benzoic acid biosynthesis in plants. *Proceedings of the National Academy of Sciences, USA* **109**: 16383–16388.

Rende U, Wang W, Gandla ML, Jönsson LJ, Niittyl T. 2016. Cytosolic invertase contributes to the supply of substrate for cellulose biosynthesis in developing wood. *New Phytologist* **214**: 796–807.

Roach M, Arrivault S, Mahboubi A, Krohn N, Sulpice R, Stitt M, Niittylä T. 2017. Spatially resolved metabolic analysis reveals a central role for transcriptional control in carbon allocation to wood. *Journal Experimental Botany* **68**: 3529–3539.

Roach M, Gerber L, Sandquist D, Gorzsás A, Hedenström M, Kumar M, Steinhauser MC, Feil R, Daniel G, Stitt M *et al.* 2012. Fructokinase is required for carbon partitioning to cellulose in aspen wood. *The Plant Journal* **70**: 967–977.

Ruuhola T, Julkunen-Tiitto R. 2003. Trade-off between synthesis of salicylates and growth of micropropagated *Salix pentandra*. *Journal of Chemical Ecology* **29**: 1565–1588.

Schauer N, Steinhauser D, Strelkov S, Schomburg D, Allison G, Moritz T, Lundgren K, Roessner-Tunali U, Forbes MG, Willmitzer L *et al.* 2005. GC-MS libraries for the rapid identification of metabolites in complex biological samples. *FEBS Letters* **579**: 1332–1337.

Schrader J, Nilsson J, Mellerowicz E, Berglund A, Nilsson P, Hertzberg M, Sandberg G. 2004. A high-resolution transcript profile across the wood-forming meristem of poplar identifies potential regulators of cambial stem cell identity. *Plant Cell* **16**: 2278–92.

Si CL, Li SM, Liu Z, Kim JK, Bae YS. 2011. Antioxidant phenolic glycosides from the bark of *Populus ussuriensis* Kom. *Natural Product Research* **25**: 1396–401.

Sundell D, Street NR, Kumar M, Mellerowicz EJ, Kucukoglu M, Johnsson C, Kumar V, Mannapperuma C, Delhomme N, Nilsson O *et al.* 2017. AspWood: high-spatial-resolution transcriptome profiles reveal uncharacterized modularity of wood formation in *Populus tremula*. *Plant Cell* **29**: 1585–1604.

Svacinova J, Novak O, Plackova L, Lenobel R, Holik J, Strnad M, Dolezal K. 2012. A new approach for cytokinin isolation from Arabidopsis tissues using miniaturized purification: pipette tip solid-phase extraction. *Plant Methods* **8**: 17.

Tegeder M, Masclaux-Daubresse C. 2018. Source and sink mechanisms of nitrogen transport and use. *New Phytologist* **217**: 35–53.

Telewski FW, Aloni R, Sauter JJ. 1996. Physiology of secondary tissues of *Populus*. In: Stettler RF, Bradshaw HD, Heilman PE, Hinckley TM, eds. *Biology of Populus and its implications for management and conservation*. Ottawa, Canada: NRC Research Press, 301–323.

Tuominen H, Puech L, Fink S, Sundberg B. 1997. A radial concentration gradient of indole-3-acetic acid is related to secondary xylem development in hybrid aspen. *Plant Physiology* **115**: 577–585.

Uggla C, Magel E, Moritz T, Sundberg B. 2001. Function and dynamics of auxin and carbohydrates during earlywood/latewood transition in Scots pine. *Plant Physiology* **125**: 2029–2039.

Uggla C, Mellerowicz EJ, Sundberg B. 1998. Indole-3-acetic acid controls cambial growth in scots pine by positional signaling. *Plant Physiology* **117**: 113–121.

Uggla C, Moritz T, Sandberg G, Sundberg B. 1996. Auxin as a positional signal in pattern formation in plants. *Proceedings of the National Academy of Sciences, USA* **93**: 9282–9286.

Vanholme R, Demedts B, Morreel K, Ralph J, Boerjan W. 2010. Lignin biosynthesis and structure. *Plant Physiology* **153**: 895–905.

Vanholme R, Morreel K, Ralph J, Boerjan W. 2008. Lignin engineering. *Current Opinion in Plant Biology* **11**: 278–285.

Wang M, Carver JJ, Phelan VV, Sanchez LM, Garg N, Peng Y, Nguyen DD, Watrous J, Kapono CA, Luzzatto-Knaan T *et al.* 2016. Sharing and community curation of mass spectrometry data with Global Natural Products Social Molecular Networking. *Nature Biotechnology* **34**: 828–837.

Weng JK, Li X, Stout J, Chapple C. 2008. Independent origins of syringyl lignin in vascular plants. *Proceedings of the National Academy of Sciences, USA* **105**: 7887–92.

Widhalm JR, Dudareva N. 2015. A familiar ring to it: biosynthesis of plant benzoic acids. *Molecular Plant* **8**: 83–97.

Wildermuth MC. 2006. Variations on a theme: synthesis and modification of plant benzoic acids. *Current Opinion in Plant Biology* **9**: 288–296.

Ye ZH, Zhong R. 2015. Molecular control of wood formation in trees. *Journal of Experimental Botany* **66**: 4119–4131.

Zinkgraf M, Liu L, Groover A, Filkov V. 2017. Identifying gene coexpression networks underlying the dynamic regulation of wood-forming tissues in Populus under diverse environmental conditions. *New Phytologist* **214**: 1464–1478.

Supporting Information

Additional Supporting Information may be found online in the Supporting Information section at the end of the article.

Fig. S1 Overview of the analytical protocol.

Fig. S2 Strategy for metabolite annotation of mass features from liquid chromatography–mass spectrometry LC-MS analysis of sample extracts from wood forming zones from five 47-yr-old aspen trees.

Fig. S3 Fiber and ray cell sample preparation of developing wood from radial sections of *Populus tremula*.

Fig. S4 Metabolite profiling by gas chromatography–mass spectrometry (GC-MS) of wood forming zones from five 47-yr-old aspen trees.

Fig. S5 Candidate gene for a precursor of salicortin biosynthesis.

Fig. S6 Expression of glutamine synthase (GS) in the wood forming tissues of four aspen trees (http://aspwood.popgenie.org/).

Methods S1 Ray and fiber preparation.

Methods S2 Metabolite extraction.

Methods S3 Plant hormone analysis.

Table S1 Metabolite profiling by gas chromatography–mass spectrometry (GC-MS) of wood forming zones from five adult aspen trees.

Table S2 Metabolite profiling by liquid chromatography quadrupole time-of-flight mass spectrometry (LC-QTOF-MS; positive ion mode) of wood forming zones from five adult aspen trees.

Table S3 Metabolite profiling by liquid chromatography quadrupole time-of-flight mass spectrometry (LC-QTOF-MS; negative ion mode) of wood forming zones from five adult aspen trees.

Table S4 Annotation of metabolites detected by liquid chromatography–mass spectrometry (LC-MS) across the wood forming tissues.

Table S5 Metabolite profiling by liquid chromatography quadrupole time-of-flight mass spectrometry (LC-QTOF-MS) of ray and fiber cells from aspen wood.

Table S6 Plant hormone concentrations in wood forming zones from five adult aspen trees.

Please note: Wiley Blackwell are not responsible for the content or functionality of any Supporting Information supplied by the authors. Any queries (other than missing material) should be directed to the *New Phytologist* Central Office.